

Reproduced by

DOCUMENT SERVICE CENTER

ARMED SERVICES TECHNICAL INFORMATION AGENCY

U. B. BUILDING, DAYTON, 2, OHIO

REEL-C

6269

A. T. I

1551231

"NOTICE: When Government or other drawings, specifications or other data are used for any purpose other than in connection with a definitely related Government procurement operation, the U.S. Government thereby incurs no responsibility, nor any obligation whatsoever; and the fact that the Government may have formulated, furnished, or in any way supplied the said drawings, specifications or other data is not to be regarded by implication or otherwise as in any manner licensing the holder or any other person or corporation, or conveying any rights or permission to manufacture, use or sell any patented invention that may in any way be related thereto."

UNCLASSIFIED

UNCLASSIFIED

ATI 155 123

(Copies obtainable from ASTIA -DSC)

U.S. Naval Ordnance Lab., White Oak, Md.

A High Speed Recording System Using the Velocity Method to Determine  
the Peak Pressure Produced in Air by Explosives - and Appendix

Kalavski, Paul Z. 25 Feb '51 34pp. photos, table, diagrs, graph

Bureau of Ordnance, Wash., D.C. (Navord Report 2167)

Recorders, Pressure-time  
Shock waves, Ballistic

Ordnance and Armament (22)  
Testing (14)

UNCLASSIFIED

**NAVORD REPORT**

2167

ASTIA FILE COPY

ATI No. 155/23

A HIGH SPEED RECORDING SYSTEM USING  
THE VELOCITY METHOD TO DETERMINE  
THE PEAK PRESSURE PRODUCED IN  
AIR BY EXPLOSIVES

25 February 1952



**U. S. NAVAL ORDNANCE LABORATORY**  
**WHITE OAK, MARYLAND**

FOR PERMANENT RETENTION

BY \_\_\_\_\_

5-484

7

NAVORD Report 2167

A HIGH SPEED RECORDING SYSTEM USING  
THE VELOCITY METHOD TO DETERMINE  
THE PEAK PRESSURE PRODUCED IN  
AIR BY EXPLOSIVES

Prepared by:  
Paul Z. Kalavski

Approved by: E. M. FISHER, Chief  
Field Shock Phenomena Division

C. J. ARONSON, Acting Chief  
Explosion Effects Division

ABSTRACT: This report has been written to describe a High Speed Recording System for determining peak pressures in the 5-90 psi pressure range from explosions in air by the velocity method. This equipment is now in use in the Mobile Air Blast Laboratory at Stump Neck, Maryland.

A brief review is given of the theoretical basis for determining peak pressure by measurement of shock and sound velocities. A description is given of the function of each component of the equipment, from the gauge to the camera. The chronological sequence of events is described. A typical record is illustrated and the method of analysis is described. Circuit diagrams are included for all units of the recording system. The accuracy limitations of the recording system are discussed.

The average standard deviation using this equipment varies from two per cent at low pressures to seven per cent at high pressures. Based on the operation of this velocity recording system, suggestions for future improvements are included.

Explosives Research Department  
U. S. Naval Ordnance Laboratory  
White Oak, Maryland



25 February 1952

NAVORD Report 2167

This report was prepared under task number NOL-Re2c-2-1-52 as a description of the instrumentation used for measuring pressure by the velocity method at the Naval Ordnance Laboratory's air blast field station at Stump Neck, Maryland.

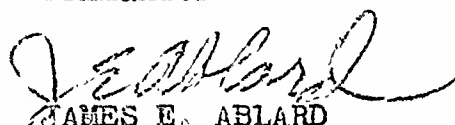
This equipment is a modified version of that designed and installed aboard the EPCS 1413 by Dr. Harry H. Hall, and described in reference (a). The present equipment was installed aboard the air blast trailer by Mr. Carl Reynolds, III and William J. Donley under the supervision of Mr. E. M. Fisher.

The author is especially indebted to Mr. Donley for his detailed analysis of the sequence of operation of various components of this equipment and to Mr. E. M. Fisher who initiated this report and aided in writing various portions of it.

The detailed analysis of the operation of individual components of this equipment was necessitated because this report will be used as a maintenance manual by those operating the equipment. Those desiring merely a general description may omit these detailed portions.

The findings represented herein are the opinions of the author and are not necessarily the opinions of the Naval Ordnance Laboratory.

W. G. SCHINDLER  
Rear Admiral, USN  
Commander

  
JAMES E. ABLARD  
By direction

# CONTENTS

|   | Page |
|---|------|
| I. Introduction . . . . .   | 1    |
| II. Basic Consideration . . . . .   | 1    |
| III. Experimental Set-up . . . . .  | 3    |
| IV. Operation of Equipment . . . . .  | 4    |
| A. General Description . . . . .  | 4    |
| B. Firing Circuits . . . . .  | 5    |
| C. Dual Time Delay . . . . .  | 5    |
| D. Preamplifier . . . . .   | 6    |
| E. Du Mont 247 Cathode-Ray Oscillograph . . . . .   | 6    |
| F. Recorder . . . . .   | 6    |
| G. Control Unit . . . . .   | 7    |
| H. Timing Indices . . . . .   | 8    |
| I. Shutter Control . . . . .  | 10   |
| V. Record Analysis . . . . .  | 10   |
| VI. Reproducibility . . . . .   | 11   |
| VII. Appendix - Derivation of the Rankine-Hugoniot Equation<br>Relating the Peak Pressure of a Shock Wave with its<br>Velocity of Propagation . . . . . | 13   |

# ILLUSTRATIONS

|  |    |
|--|----|
| Figure 1. Instrument Hut and Transit Platform at<br>Stump Neck, Maryland . . . . .   | 17 |
| Figure 2. Relative View of Hut, Trailer and Field . . . . .  | 18 |
| Figure 3. Position of Gauges, Detonator Caps and<br>Charge . . . . .   | 19 |
| Figure 4. Spacing the Gauges . . . . .   | 20 |
| Figure 5. Diagram of Field Set Up Showing Cable<br>Connections . . . . .   | 21 |
| Figure 6. Inserting the Firing Jumper thereby<br>joining the Field Firing Cables into<br>Firing Channels . . . . .             | 22 |
| Figure 7. Block Diagram of High Speed Recording<br>Equipment . . . . .   | 23 |
| Figure 8. Cap Firing Circuit . . . . .   | 24 |
| Figure 9. Dual Time Delay Schematic Circuit . . . . .  | 25 |
| Figure 10. Charge Firing Schematic Circuit . . . . .   | 26 |
| Figure 11. Front View of Firing and Dual Time Delay<br>Panels . . . . .  | 27 |
| Figure 12. Photograph of High Speed Recorder and<br>Associated Equipment . . . . .   | 28 |
| Figure 13. Preamplifier Schematic Circuit . . . . .  | 29 |
| Figure 14. High Speed Recorder and Oscillograph<br>Showing Hole Through which Crate Tube Flashing<br>is Photographed . . . . . | 30 |

# NAVORD Report 2167

## ILLUSTRATIONS

|   | Page |
|---|------|
| Figure 15. Drum Film Holder . . . . .   | 31   |
| Figure 16. Control Unit Schematic Circuit . . . . .   | 32   |
| Figure 17. Pulse Generator Schematic Circuit. . . . .   | 33   |
| Figure 18. Typical Record Indicating Arrival Times of<br>Signal from Detonator Caps and Charge. | 34   |

## I. INTRODUCTION

1. Investigations of the properties of explosions in air are made by recording the pressure time curve or the parameters of the pressure-time curve, such as peak pressure and positive impulse. The techniques for measuring the blast parameters involve the use of mechanical and electrical gauges.
2. Mechanical gauges, though much simpler than electrical gauges, have not been developed to the point where pressure-time curves can be recorded with adequate fidelity.
3. The electrical methods depend on the measurement of an electrical signal, due to mechanical displacement produced by the pressure wave in the elements of a pressure-sensitive pick-up.
4. Certain classes of crystals, when subjected to mechanical stress, have the property of developing electrical charge on various crystal faces. Such crystals are called "piezoelectric". Piezoelectric gauges have been used by most laboratories engaged in air blast work (reference c), and are being used here at the Naval Ordnance Laboratory. Tourmaline has been used exclusively, although others such as barium titanate are now being considered.
5. Pressure measurements which are determined directly by a gauge are, in general, affected by the distortion in the pressure field caused by the presence of the gauge in the path of the shock wave. Consequently these gauges do not record the "true" pressure in the blast wave.
6. However, a much better indication of the "true" pressure in a shock front may be determined by measuring the speed of propagation of the front in a direction normal to itself. Inasmuch as shock-velocity measurements are not affected by the distortion of the shock with the measuring devices, pressures determined this technique are called "true" pressures as distinguished from the pressures measured directly by a pressure sensitive gauge.

## II. BASIC CONSIDERATIONS

7. The relation between the velocity of propagation and the pressure in a shock wave is obtained from the Rankine-Hugoniot equations and the properties of the medium. The Rankine-Hugoniot equations are based on the conservation of mass, momentum, and energy across the shock front. By assuming that the ratio of the specific heat at constant pressure to that at constant volume is a constant across the shock front, and by assuming that air obeys the ideal gas law, it is possible to derive the equation

$$\frac{P_s}{P_o} = \frac{2\gamma}{\gamma+1} \left[ \left( \frac{U^2}{c_o^2} - 1 \right) \right]$$

(See appendix for derivation)

Where:

- $P_s$  = peak pressure in the shock front in excess of atmospheric pressure  
 $P_o$  = atmospheric pressure  
 $U$  = velocity of propagation of shock front  
 $c_o$  = speed of sound in undisturbed air  
 $\gamma$  = ratio of specific heat at constant pressure to specific heat at constant volume (1.40 for air).

8. All measurements of peak pressure by the velocity method have been calculated using this equation. To determine the shock pressure  $P_s$  it is necessary to evaluate the shock velocity  $U$ , the sound velocity  $c_o$ , and to know the barometric pressure  $P_o$ . However since  $U$  is the shock velocity relative to the medium, motion of the air (wind) leads to an incorrect measurement of  $U$  by stationary devices. Therefore the instantaneous wind velocity must also be determined. In addition, inasmuch as the shock velocity is measured over a finite interval, it is necessary to evaluate the distance from the explosion at which the average shock velocity over the interval of measurement is equal to the instantaneous velocity.

9. The speed of sound is determined by using as sources of sound two detonator caps, one at each end of the line of velocity gauges. However, because of the effect of wind velocity, the apparent sound and shock velocities as measured on the records are in error. If  $c_o$  is true sound velocity,  $c_1$  the apparent sound velocity as measured from detonator cap #1, and  $c_2$  the apparent sound velocity measured using detonator #2, we get

$$c_1 = c_o + W \cos \theta$$

$$c_2 = c_o - W \cos \theta$$

where  $\theta$  is the angle the wind makes with respect to the line of velocity gauges and  $W$  is the velocity of the wind.

Adding the two equations gives the true sound velocity

$$c_o = \frac{c_1 + c_2}{2}$$

Subtracting the two equations gives the component of the wind velocity in the direction of the line of gauges or

$$W \cos \theta = \frac{c_1 - c_2}{2}$$

This latter correction must be applied to the apparent shock velocity measurement to give the "true" shock velocity.

If no wind is present, the speed of sound  $c$  can be obtained from the measurement of the air temperature by using the formula

$$c = c_0 \left( 1 + \frac{t}{273} \right)^{\frac{1}{2}}$$

Where:

$c$  = speed of sound in dry air at temperature  $t$

$c_0$  = speed of sound in dry air at  $0^\circ\text{C}$  (1088.3 ft/sec used)

$t$  = temperature of air in degrees centigrade

10. In using this latter method, the effect of humidity on the speed of sound must be taken into consideration. The variation of the speed of sound with humidity is given by

$$c_m = c_d \left( 1 + 0.149 \frac{P_w}{P_a} \right)$$

Where:

$c_m$  = speed of sound in moist air

$c_d$  = speed of sound in dry air

$P_w$  = partial pressure of water vapor

$P_a$  = partial pressure of air

11. When the speed of sound is determined by the measurement of the velocity of a small-amplitude shock wave, humidity affects the calculated pressures only through its effect on  $\gamma$ , the ratio of specific heats of air, since  $U$ ,  $c$ , and  $P_0$  are measured quantities at the particular value of humidity. At 100% humidity the correction to  $\gamma$  is 0.3 per cent and the maximum error in the shock pressure due to this 0.3 per cent error in  $\gamma$  is only .13 per cent, as can easily be seen when substituted in original Rankine-Hugoniot equation. Therefore humidity has an entirely negligible effect when the speed of sound is determined by velocity measurements.

### III. EXPERIMENTAL TECHNIQUE

12. A pictorial view of the experimental facilities may be seen in figures 1 and 2. In order to measure the shock wave velocity  $U$ , nine piezo-electric gauges were placed along a straight line, perpendicular to the shock front and at measured distances from the charge. The position of the charge and detonators with respect to the line of velocity gauges are indicated in figures 3, 4 and 5. The signal from each gauge is recorded by an oscillograph and rotating drum camera. In order to obtain as short a rise time

as possible, the gauges are placed "face-on" to the blast.

13. The speed of sound is determined by using the same line of gauges as is used for shock wave velocity and using two detonator caps as the source of sound, one at each end of the line of gauges. The two caps and charge are detonated approximately 30 ms apart. This technique is used primarily because it permits the determination of the wind velocity at or near the instant of the explosion.

#### IV. OPERATION OF EQUIPMENT

##### A. General Description of Equipment.

14. Figure 7 is a block diagram showing the interconnection of the various units comprising the high-speed recording equipment. Figure 8, 9, and 10 are schematic diagrams of the cap firing, time delay, and charge firing circuits. Figure 11 shows a pictorial view of the front of the chassis containing the above circuits.

15. After the pulse from the first firing circuit trips the beam brightening circuit in the Du Mont 247 oscilloscope, the beams remain on for approximately 90 milliseconds. Since the time intervals between the firing of the two caps and between the second cap and charge is 30-35 ms, this 90 ms duration is adequate.

16. The timing control unit generates the millisecond pulses used for measuring time. This unit remains on for only one revolution of the drum camera, or approximately 30-35 ms.

17. In order to get a separate trace for the entire length of film for each charge and each cap, without superimposing the traces, the position of the spot on the oscilloscope is displaced before the 2nd cap and again before the charge is fired. This is accomplished by the dual time delay energizing the relays which remove a resistor in the grid circuit of the positioning tube in the Du Mont oscilloscope, thereby displacing the spot first to the center for the second cap, then to the bottom of the film for the charge (figure 18).

18. When the firing switch  $S_1$  is closed, the first thyatron tube  $V_2$  in the cap firing circuit is fired, producing a pulse through transformer P6134, and thence simultaneously into the beam brightening circuit of the Du Mont 247 oscilloscope and the trip input of the dual time delay. The output of the strobotron tube  $V_3$  fires blasting cap #1. The output of the first time delay operates both the relay which displaces the beam on the oscilloscope and the relay which fires the second cap. The pulse output from the second time delay operates the attenuator in the preamplifier, the second displacement relay, the timing control unit, and the charge firing circuit.

## B. Firing Circuits.

19. The purpose of a firing circuit is to provide a pulse of sufficient voltage to fire a detonator. Except for minor differences, the two cap-firing circuits and the charge-firing circuit are identical. The three circuits differ only in their manner of being actuated.

20. The firing circuits, shown schematically in figures 8 and 10, consist essentially of a 2050 thyatron, an SN4 strobotron and a self-contained power supply providing plate and heater voltages for these tubes.

21. The reset switch is normally closed. When this switch is pushed and then released, the plate supply voltage is removed and then reapplied to the two gas tubes. In the reset position, the biases are such that the tubes cannot fire until an additional pulse is applied. When the cap firing switch  $S_1$  is closed, the cathode resistor in the thyatron of the first cap firing circuit is shorted, thereby firing the tube and sending a pulse simultaneously to the beam brightener circuit of the Du Mont 247 Oscilloscope and the trip input of the Dual Time Delay. The output of the strobotron fires the detonator.

## C. Dual Time Delay.

22. The function of the Dual Time Delay is to control the sequence of and time intervals between various operations including the turning on and off of the timing unit, the firing of the charge and 2nd cap and the displacement of the spots on the oscillograph.

23. This unit, shown in figure 9, consists of a 6SL7 twin triode, three 2050 thyatrons, and a self-contained power supply providing a plus 255 volts and a negative 105 volts. The two Cornell-Dubilier decade condensers in series with the 3.9 megohm resistors give the time delay required for the various operations involved.

24. The pulse output from the first cap-firing circuit fires the first thyatron which in turn actuates the timing unit by means of the Sigma relay in the cathode. Approximately thirty-three milliseconds later, as determined by the 1st time delay, the second thyatron fires, the beams are displaced and the 2nd cap circuit is actuated. Another thirty-three milliseconds later, as determined by the second time delay, the third thyatron fires, actuating the charge-firing circuit, the second displacement and the relay which cuts off the timing. In addition this tube actuates the relay in the output of the preamplifier which attenuates the signal from the charge.



#### D. Preamplifier

25. The preamplifier, shown pictorially in Figure 12 and schematically in Figure 13, is a low-gain two-stage amplifier, consisting of a cathode biased 6SJ7 sharp cut-off pentode and a 6J5 medium-mu triode used as a cathode-follower. In the input there is a potentiometer which controls the amount of signal applied to the grid. In the output there is an attenuator controlled by a Sigma relay which is energized by the dual time-delay unit, after a predetermined time interval. This attenuator and relay is necessary because of the need for rapidly changing from high gain in recording the sound from the blasting cap, to low gain for the shock wave velocity produced by the charge.

26. The signals from the two blasting caps pass through the preamplifier to the Du Mont 247 oscilloscope with no attenuation. Approximately 60 ms after the beam brightening circuit is tripped, the Sigma relay closes and the attenuator is inserted just before the signal from the charge enters the preamplifier.

#### E. Du Mont 247 Cathode-Ray Oscillograph

27. The type 247 Cathode-Ray Oscillograph is shown in figures 12 and 14. It is an instrument for plotting a visual curve of one electrical quantity as a function of another on the screen of a cathode-ray tube. It consists essentially of a cathode-ray tube, amplifiers for producing the deflection voltages, and a linear time-base generator, and associated power supplies.

28. In addition to being deflected vertically and horizontally, the electron beam may be modulated in intensity. The Y-axis or vertical deflection amplifier has uniform frequency response within 3db from 1/2 cps to 300 kc.

29. This oscillograph has been altered in the grid circuits of the positioning stage in order to provide the displacement of the beam position for the charge and each cap signal. For detailed analysis of its operation see the operating and maintenance manuals published by the Allen B. Du Mont Laboratories.

#### F. Recorder

30. The recorder as now used on the trailer is shown in Figures 12 and 14 and consists of a recorder hood, lens assembly and rotating drum film holder and shutter for recording with moving film. The hood, made of welded sheet steel, is mounted over the face of the cathode-ray oscilloscope. The lens assembly is mounted in the hood. The lens tube can be extended and clamped in focussed position. The shutter and film holding parts of the recorder are separate, easily detached assemblies. Mounted within the hood and to one side, is an electrically operated counter, an image of whose face is reflected by two small mirrors, into the field of the recorder lens, in the plane of the oscilloscope screen.

The characters of the counter are illuminated by two small lamps, timed manually, to give a suitable exposure of the counter face upon the film record for identification purposes. The entire hood assembly is hinged, and may be opened to allow access to the counter and the face of the cathode ray tube.

31. The Drum Film Holder is shown in Figure 15. A strip of 35 mm film about 18 inches long is carried on the surface of an aluminum drum 5.3 inches in diameter. The film is retained on the drum by an outer band of lucite. This band is under-cut so that the film can be slipped between it and the drum surface, through a slot in the drum's metal rim. When the drum rotates, the film is pressed against the lucite by centrifugal reaction and is thus held accurately in position. The drum is carried on the shaft of a small motor. An 1800 rpm synchronous motor is used giving a linear speed of the film of about 500 inches per second.

#### G. Control Unit.

32. The control unit, shown above the recorder hood in Figure 12 and schematically in Figure 16 is operated by relay circuits from a single master control, and which in turn controls the functions of its own recording channel. This unit provides, in addition, the local power at each channel for various operations, e.g. opening and closing the recorder shutters, illuminating the electric counter whose numerals are photographed on the record, and flashing the gas discharge tube which applies the timing indices.

33. Each control function can also be initiated at the channel by means of a key. These keys make possible the manual operation of the channel for experimental or maintenance purposes. The recorder motor control and shutter keys, with their associated relays, light red panel lamps when operated. These indicate proper operation of the relay circuits and also warn the operator to return all locking controls to normal position when preparing for remote operation. Other panel lamps are green. Thus, when the channel is ready for operation, no red panel lights should appear.

34. If no camera, or a fixed camera, is plugged into the control unit, a base line with 1000 cycle pips appears on the oscilloscope, when base line key is depressed or base line relay is actuated. This feature of the equipment is not used in the application under discussion in this report. With a rotating drum camera in place on the control unit, depressing base line key or actuating base line relay applies a base line on the oscilloscope without pips.

Reason: On rotating drum camera plug, pins 2 and 3 are shorted, and pins 4 and 5 are shorted. Thus, -300V is applied to the plate of  $V_3$  preventing it from firing. (-300V to pin 4, to pin 5 through short in camera plug; to common of timing relay, to timing relay, to normally closed of timing key; to normally closed of timing relay; through 50 K to plate of  $V_3$ ). When the base line key is depressed, it applies 30-cycle pulses to the grids of  $V_1$  and  $V_2$  allowing these tubes to fire and it also removes the shorting ground from the 5K ohm resistors from which the triggering pulse is obtained for use in the scope. When  $V_1$  fires it applies a voltage across these now ungrounded resistors and the resulting voltage goes out to brighten the beam of the oscilloscope.

35. With no camera, (or fixed camera), the -300 volts is removed from the plate of  $V_3$  and the short across the two 5K ohms resistors is removed, so that when the base line key or relay is actuated and 30-cycle pulses applied to the flasher circuit, a base line with pips appears on the oscilloscope. When the timing key or relay is actuated, no signal appears on the oscilloscope when the rotating drum camera is in place because the two 5K ohm resistors producing the beam brightening pulse are shorted to ground.

#### H. Timing Indices.

36. A General Radio vacuum tube driven fork oscillator is used to produce a 1000-cycle signal, accurate to within .1%. This signal is converted into 1000-cycle pulses, of a few microseconds width, by one channel of a pulse generator shown in Figure 17. The signal is alternately amplified and clipped by a series of four triodes ( $V_5$  and  $V_6$ ) operating at zero bias, resulting in a 1000-cycle square wave. This is coupled by a differentiating circuit to the grid of an amplifier,  $V_7$ , which drives a cathode-follower impedance matching stage. The output consists of 70-volt pulses which are applied to the crater tube circuits in the control unit. The pulse generator further contains a generator of 30-cycle pulses derived from the power frequency, and therefore synchronized with the revolutions of the drum recorder, which revolves at 30 rps. The 60-cycle line voltage is applied first to an unbiased amplifier  $V_1$ , which clips the negative swings. This is coupled through an .001 mfd condenser, which, by differentiating the signal, applies sharp 60-cycle pulses to a multivibrator,  $V_2$ , operating at 30-cycles. The 30-cycle pulses from the multivibrator are differentiated by the coupling circuit to the unbiased amplifier,  $V_3$ , which clips the negative peaks, and amplifies the positive ones.

37. The timing signals, required for use in the drum recorder, are a series of short flashes occurring at millisecond intervals, lasting just long enough to go once around the recorder drum. Running at 1800 rpm the drums turn once in  $33 \frac{1}{3}$  milliseconds.

Thus a series of 33 flashes are required. To initiate these flashes, 30-cycle pulses derived from the line frequency, and 1000-cycle pulses controlled by the fork oscillator, are supplied by the pulse generator. A gas-discharge crater tube (Sylvania R1130) is connected in series with a thyratron 2050,  $V_4$ , (Figure 16) across a 125 mfd condenser which is charged to 300 volts by the power supply.  $V_4$  is fired by each of the 1000-cycle pulses, causing the crater tube to flash, and is extinguished by its rising cathode potential, due to the charging of a .01 mfd series condenser in its cathode return. The charge on this condenser leaks off through 25,000 ohms before the next pulse occurs one millisecond later. To prevent continued flashing of  $V_4$  and the crater tube, the screen of  $V_4$  is biased strongly negative. To allow a series of flashes, the bias is removed for  $1/30$  second. This is accomplished by applying the 30 cycle pulses to the two thyratrons,  $V_1$  and  $V_2$ , by closing a key or the relay  $R_3$ . Initially, there is no potential between the cathode and plate of  $V_2$ , so that only  $V_1$  fires. The charge on condenser  $C_1$  then flows through  $V_1$  to  $C_2$ , until  $V_1$  is extinguished by the rising potential of  $C_2$ . There is now a potential across  $V_2$  while that of  $V_1$  is too small for firing. The next pulse fires  $V_2$ , returning  $C_1$  to nearly its original potential, while  $C_2$  slowly discharges through its 2-megohm shunt. This discharge is slow enough to keep  $V_1$  from again firing until one or two seconds have passed, which allows ample time for the relay  $R_3$  to be reopened. Thus, closure of  $R_3$  applies the 30 cycle pulses to  $V_1$  and  $V_2$ , and causes one negative square pulse, lasting  $1/30$  second, to be applied to the grid of  $V_3$ , which in turn removes the negative bias on the screen of  $V_4$  for the desired time.

38. Quiescent State: 1000-cycle pulses are continuously applied to grid of  $V_4$ . This tube cannot fire because its screen grid is held down to approximately -150V as long as  $V_3$  is conducting. When  $V_4$  fires, flasher tube Sylvania R1130 fires, flashing at a 1000-cycle rate.

39. When 30-cycle pulses are applied, they go to the control grids of  $V_1$  and  $V_2$ . However only  $V_1$  can fire on the first 30-cycle pulse because  $V_2$  has both its cathode and plate at  $B^+$  potential (300V) and therefore effectively zero potential across it, while  $V_1$  has the full 300V supply across it.

40. Dynamic Operation: (1) a 30-cycle pulse is applied to control grids of  $V_1$  and  $V_2$  through relay. (2) Only  $V_1$  fires (see above). High side of 270-ohm resistor in plate circuit of  $V_1$  drops from 300V to 150V, putting a 150-volt negative pulse on the grid of  $V_3$  causing the plate of  $V_3$  to rise to ground potential; this ground potential is therefore applied to the screen of  $V_4$ .

(3) With screen at ground, 1000-cycle pulses on grid of  $V_4$  fires this tube, which in turn fires Sylvania R1130 giving 1000-cycle flashes. (4) When high side of 270 ohm resistor drops to 150V, a 150 V drop appears across  $V_2$  setting this tube up for firing. Also  $C_1$  drops to 150V and  $C_2$  charges up to 150V. The latter condenser, charging up to 150V, applies this voltage to the cathode of  $V_1$ , extinguishing this tube. (5) When the second 30-cycle pulse appears on the grids of  $V_1$  and  $V_2$ ,  $V_1$  cannot fire because  $C_2$  is still charged to 150V, putting zero potential effectively across  $V_1$ .  $V_2$  fires and raises high end of 270 ohms resistor back to 300V. This allows  $V_2$  to conduct once more, bringing its plate voltage down to -150V which is applied to the screen of  $V_4$ , shutting  $V_4$  off. Thus a -150 volt signal is applied to  $V_3$  for 1/30th sec., which in turn allows  $V_4$  to fire for 1/30th sec. (6) When  $V_2$  fires it practically shorts the 1 meg. resistor across it, which moves the cathode of  $V_2$  to B+ potential, extinguishing the tube. (7)  $V_1$  will not fire until  $C_2$  discharges through the 2 meg. resistor. This takes about 2 seconds.

## I. Shutter Control

41. The Shutter Control is located in, but unrelated to the "Control Unit". A relay, paralleled by a key marked "Shutter", closes a circuit through the shutter-operating solenoid of the recorder. This circuit is powered by a small power transformer, T6, and a selenium rectifier, shunted by a large electrolytic condenser of 1000 mfd, as shown in Figure 16. On closure, the condenser, which has been charged to the peak value of the applied voltage, discharges through the solenoid, providing a strong actuating impulse. When the shutter-actuating plunger has been drawn into the solenoid, a small current suffices to hold the shutter open. Thus, the steady current supplied by the rectifier, (which is much less than the initial current surge because the voltage falls to its average value), can hold the shutter open until it is released by the relay or key. A small, compact solenoid, which would be burned out by the current necessary to actuate the shutter, were it applied continuously, can thus be used.

## V. RECORD ANALYSIS

42. The 35 mm film record to be analyzed is approximately 18 inches in length. A typical velocity record is shown in figure 18. The vertical lines are millisecond timing marks. The lines of sharp pips are the signals recorded by the gauges. They are numbered so as to correspond with the velocity gauge producing them. To facilitate identification some of these marks are made positive and others negative.

This is done by using positive and negative gauges. It may be observed that there are three lines of sharp pips on the film. The first line is produced by the first blasting cap, the second line by the second blasting cap and the bottom line contains those pips produced by the charge.

43. These records are placed in a microfilm reader which magnifies the record approximately fifteen times and projects it on the cross section paper placed below it. The location of the pips are then marked on the cross section paper. The pips are read at the point where they first leave the base line at the most rapid rate. These distances on the coordinate paper are then measured using the 50th divisions on an engineer's scale, and then converted into arrival time. With this enlargement it is possible to divide the time axis into one microsecond intervals. Dividing this arrival time into the known distances between the appropriate gauges gives the average velocity between these gauges. We then may plot a curve showing the velocity as a function of the distance. In addition, the apparent sound velocity both up and down the line of gauges is determined; from which we can calculate the component of the wind velocity along the line of gauges and the true sound velocity. This wind velocity correction is then applied to the shock wave velocity.

44. The speed of sound in free air can also be computed from tables if the temperature, relative humidity, and barometric pressure is known. However, this does not include the wind velocity correction. The peak pressure at the midpoint of the distance between two gauges is then determined using the Rankine Hugoniot equations for ideal gases, as given in introduction, and derived in the appendix.

## VI. REPRODUCIBILITY

45. The peak pressures produced by 8-pound spherical TNT charges were 6-90 psi for the various distances used in the field. Since many explosives have been fired using this equipment, a measure of the precision of this equipment would be indicated by a measure of the dispersion of the results, assuming the explosive does not contribute to the scatter significantly. An average of all the standard deviations was used for this purpose. This was found to be 5%. It may be observed that greater reproducibility is possible at lower pressures than at higher pressures. At the lower pressures the standard deviation often goes down to 2% but at the higher pressures the standard deviation often reaches as high as 7%.

46. However since larger distances and times are associated with lower pressures, and lower distances and times with higher pressure the above error might be attributed to the increased accuracy with which longer distances and times can be measured. To increase the accuracy with which distances between gauges are measured,



aluminum spacer gauges are used. For increased accuracy in record reading, the gauge separation distances were chosen approximately logarithmic so that equal abscissa distances on the curve are obtained. A detailed discussion of the accuracy limitations of the velocity method is beyond the scope of this report. However some of the major sources of error will be discussed.

47. Although there was some variation in the accuracy of measurement throughout an experiment, an error of .5%, .3%, and .5% in wind, time, and distance measurement is assumed. To find the errors in pressure measurements due to these errors in velocities we use the original Rankine-Hugoniot equation

$$\frac{P}{P_0} = \frac{2\gamma}{\gamma+1} \left( \frac{U^2}{C^2} - 1 \right)$$

$$\frac{P}{P_0} = \frac{2\gamma P_0}{\gamma+1} \left( \frac{U^2}{C^2} - 1 \right)$$

and

$$\Delta P = \frac{2\gamma P_0}{\gamma+1} \left( \frac{2U\Delta U}{C^2} \right)$$

$$\frac{\Delta P}{P} = \frac{\frac{2\gamma P_0}{\gamma+1} \left( \frac{2U\Delta U}{C^2} \right)}{\frac{2\gamma P_0}{\gamma+1} \left( \frac{U^2}{C^2} - 1 \right)} = \frac{2}{\left( 1 - \frac{C^2}{U^2} \right)} \frac{\Delta U}{U}$$

48. Table 1 below lists the coefficient of  $\frac{\Delta U}{U}$  for selected pressures together with errors in pressure corresponding to the errors in shock and sound velocity listed above.

TABLE I

PRESSURE ERRORS DUE TO SOUND AND SHOCK VELOCITY ERRORS

| $P_s$ (lb/in <sup>2</sup> ) | $\frac{2}{1 - C^2/U^2}$ | Maximum $\frac{\Delta U}{U}$ %<br>(For Shock and<br>Sound Velocity) | Maximum Error $\frac{\Delta P}{P_s}$ |
|-----------------------------|-------------------------|---|--------------------------------------|
| 50.                         | 2.69                    | 2.1   | 5.6                                  |
| 20.                         | 3.71                    | 2.1   | 7.8                                  |
| 5.                          | 8.86                    | 2.1   | 18.6                                 |

49. Based on the above estimates for errors in velocities, the values of maximum pressure errors become 5.6% for 50 psi, 7.8% for 20 psi and 18.6% for 5 psi. For pressures below 5 psi the error increases very rapidly. It is to be noted that the estimated errors in shock and sound velocities include experimental errors as well as variations due to explosives themselves.

50. Another possible error is the assumption that the average velocity occurs at a distance midway between two gauges. An analysis of this error is fully explained in (reference (b)). This error is small when the distance between the two gauges is small. By judicious selection of gauge separations, this error has been made negligible in our measurements.

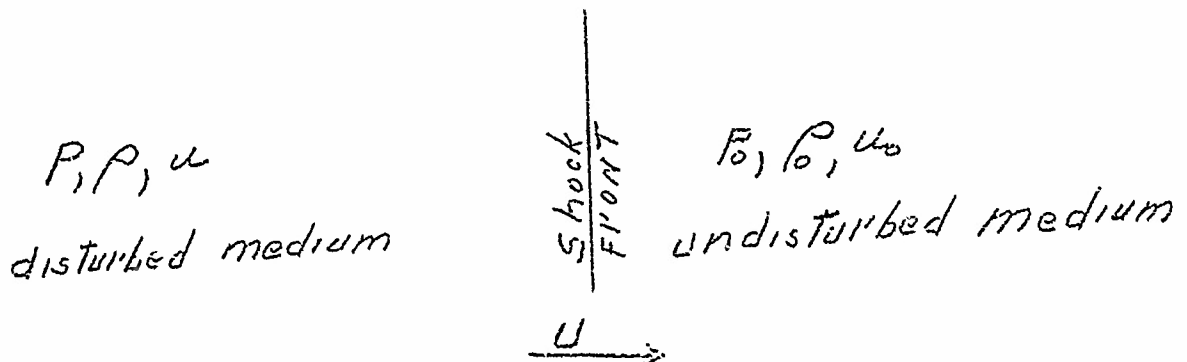
51. The pressure measurements by the velocity method may be improved by more accurate measurements of the gauge separations. At the present time these distances are measured to within .001 feet.

52. Greater precision may be obtained during record reading if the velocity of the drums were increased, because of the resultant greater separation between the timing line pips. However since this error is so small in comparison with our other errors, no further increase in drum speed is contemplated, at the present time.

# VII. APPENDIX

53. Derivation of  $\frac{P_s}{P_o} = \frac{2\sqrt{\gamma}}{\gamma+1} \left( \frac{U^2}{C_o^2} - 1 \right)$ , the Rankine-Hugoniot

Equation Relating the Peak Pressure in a Shock Wave with its Velocity of Propagation





54. If a shock wave travels with a velocity  $U$  into undisturbed air (particle velocity  $U_0$ , pressure  $P_0$ , density  $\rho_0$ ) and if the air behind the shock front is at pressure  $P$ , density  $\rho$  and particle velocity  $u$ , then for a unit mass of air crossing the shock front the applications of the conservation of mass, momentum, and energy relations will give us equations involving  $U$ ,  $P$ ,  $\rho$ ,  $U$ ,  $P_0$ ,  $\rho_0$  and  $u_0$ . These equations are known as the Rankine-Hugoniot equations. When these relations are supplemented by an equation of state and the thermodynamic properties of the fluid, a relation between the velocity of propagation and the pressure in a shock wave is obtained.

55. It is convenient to consider the parameters relative to an observer moving with the shock front. In one second the mass of the gas that crosses a unit cross section of the wave front from the undisturbed region is  $\rho_0 (U - u_0)$ . This must equal the mass that leaves from the disturbed region of the shock front  $\rho (U - u)$  in one second. Hence for conservation of mass

$$(1) \quad \rho (U - u) = \rho_0 (U - u_0)$$

56. The momentum of the mass  $\rho_0 (U - u_0)$  is  $\rho_0 (U - u_0)^2$ . Similarly the momentum of the mass  $\rho (U - u)$  is  $\rho (U - u)^2$ . The change in momentum per unit time across the shock front must equal the force acting. This force is the pressure difference on the two sides of the shock front times the cross section area of the front. For unit cross section area of the shock front, the conservation of momentum equations are:

$$(2) \quad P - P_0 = -\rho (U - u)^2 + \rho_0 (U - u_0)^2$$

or

$$(2a) \quad P + \rho (U - u)^2 = P_0 + \rho_0 (U - u_0)^2$$

57. To obtain the energy equation we need to know the internal energies of a unit mass of the gas in front of and behind the shock front. This is the work done against external pressure when the gas is expanded adiabatically to zero density. These internal energies we call  $E$  and  $E_0$ .

58. The work done by pressure per unit area per unit time on a mass of gas of unit cross section area of the wave front, is  $\frac{P}{\rho} (U - u_0) - \frac{P_0}{\rho_0} (U - u)$ . For a unit mass of the gas this becomes  $\frac{P}{\rho} - \frac{P_0}{\rho_0}$ , since  $\rho_0 (U - u_0)$  is equal to  $\rho (U - u)$ . This must equal the kinetic energy plus the change in internal energy of the gas. The kinetic energy per unit mass is given by

$K E = 1/2 [(U-u)^2 - (U-u_0)^2]$ . The change in internal energy is given by  $E-E_0$ .

Therefore

$$P_0/\rho_0 - P/\rho = 1/2 [(U-u)^2 - (U-u_0)^2] + (E-E_0)$$

or

$$(3) \quad P_0/\rho_0 + 1/2 (U-u_0)^2 + E_0 = P/\rho + 1/2 (U-u)^2 + E$$

59. If in equation 3,  $U$  and  $u$  are eliminated by using equations 1 and 2, and noting that  $u_0 = 0$  when the fluid is initially at rest, we get

$$(3a) \quad \Delta E = E - E_0 = 1/2 (P+P_0)(1/\rho_0 - 1/\rho).$$

where  $\Delta E$  is the increase in energy per gram in passing from region in advance of shock front to that immediately behind the shock front.

60. For an ideal gas  $P = K \rho^r$ , where  $\rho = 1/v$  for a unit mass of the gas. Therefore the internal energy may be calculated as follows:

$$(4) \quad E = \int_{1/\rho}^{\infty} P d(1/\rho) = \int_{1/\rho}^{\infty} K \rho^r d(1/\rho) = \int_{\rho}^{\infty} K \rho^r \frac{(-d\rho)}{\rho^2} \\ = -K \left[ \frac{\rho^{r-1}}{r-1} \right]_{\rho}^{\infty} = \frac{K \rho^{r-1}}{r-1} = \frac{P}{\rho^r} \frac{\rho^{r-1}}{r-1} = \frac{P}{(r-1)\rho}$$

Similarly  $E_0 = \frac{P_0}{(r-1)\rho_0}$

$$\therefore E - E_0 = \frac{P}{\rho(r-1)} - \frac{P_0}{\rho_0(r-1)} = \frac{P_0 + P}{2} \left( \frac{1}{\rho_0} - \frac{1}{\rho} \right) \text{ from eq. (3a)}$$

From which

$$\frac{P_0}{\rho_0} = \frac{(r-1)P + (r+1)P_0}{(r+1)P + (r-1)P_0}$$

From equation 1

$$\frac{P_0}{\rho_0} = \frac{U-u}{U} = 1 - \frac{u}{U} \quad \frac{(r+1)P_0 + (r-1)P}{(r-1)P_0 + (r+1)P} = \frac{2P - 2P_0}{(r+1)P + (r-1)P_0}$$

$$(5) \quad \frac{u}{U} = 1 - \frac{P_0}{P} = \frac{2P_0}{(r+1)P + (r-1)P_0} \quad \text{Where } P_0 = P - P_0$$

Another relation between  $u$  and  $U$  may be obtained by multiplying equation (1) by  $U-u$

$$(U-u)^2 \rho = U(U-u) \rho_0$$

Substituting this in equation 2 we get

$$P - P_0 = P_s = \rho_0 U^2 + \rho_0 U u - \rho_0 U^2 = U u \rho_0$$

and

$$U u = \frac{P_s}{\rho_0}$$

but  $C_0^2 = \frac{V P_s}{\rho_0}$  where  $C_0$  is the sound velocity

$$(6) \therefore U u = \frac{C_0^2 P_s}{V \rho_0}$$

Dividing equation 6 by equation 5 we get

$$\frac{U u}{\frac{U}{U}} = U^2 = \frac{\frac{C_0^2 P_s}{V \rho_0}}{\frac{2 P_s}{(r+1) P_s + (r-1) P_0}} = \frac{C_0^2}{2 V} \left[ \frac{(r+1) P}{P_0} + (r-1) \right]$$

But  $P = P_s + P_0$

$$\therefore \frac{P_s}{P_0} = \frac{2 V}{r+1} \left[ \frac{U^2}{C_0^2} - 1 \right]$$

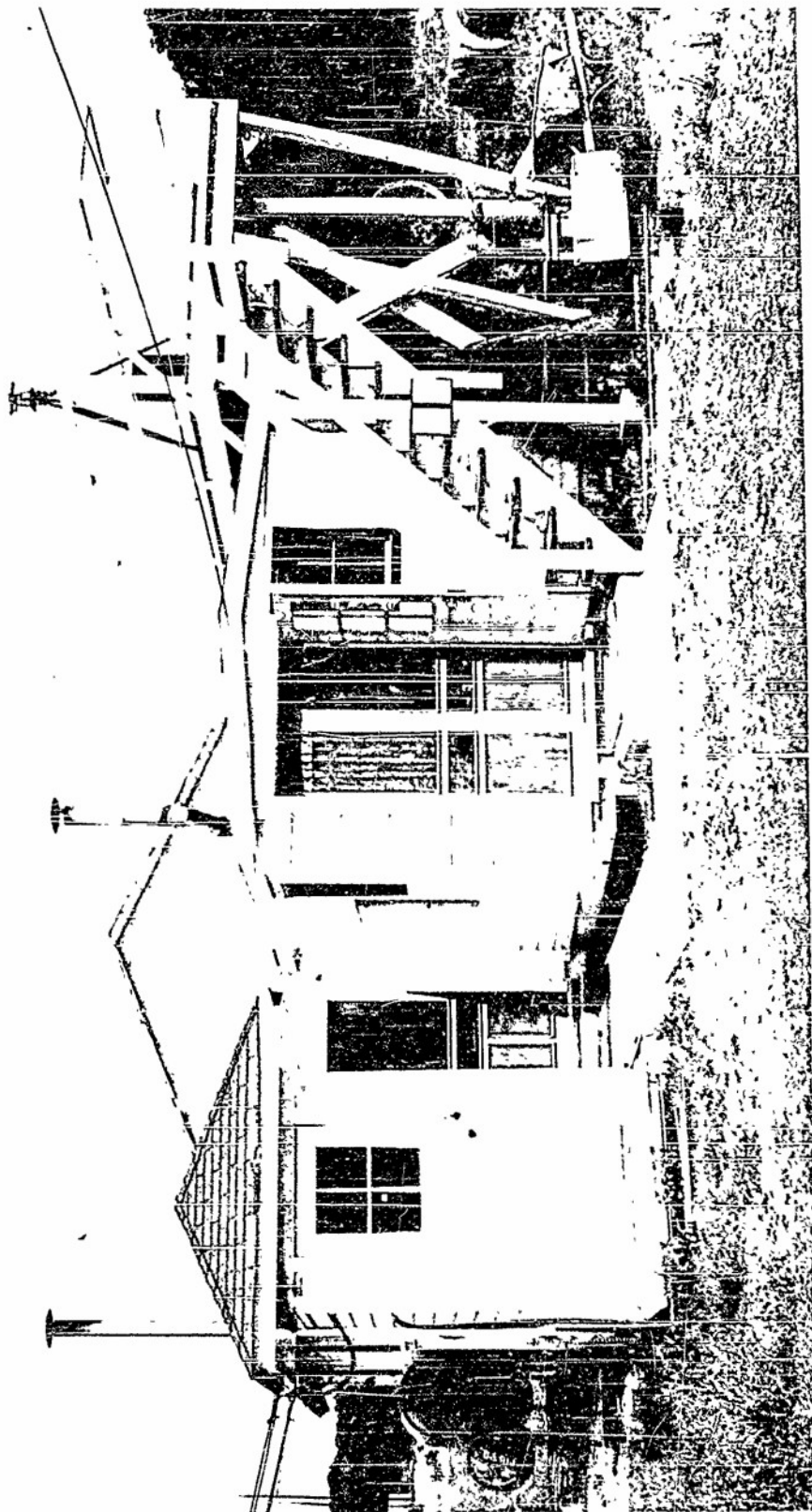


FIG. 1  
INSTRUMENT HUT AND TRANSIT PLATFORM AT STUMP NECK, MARYLAND



FIG. 2  
VIEW OF HUT, TRAILER AND FIELD

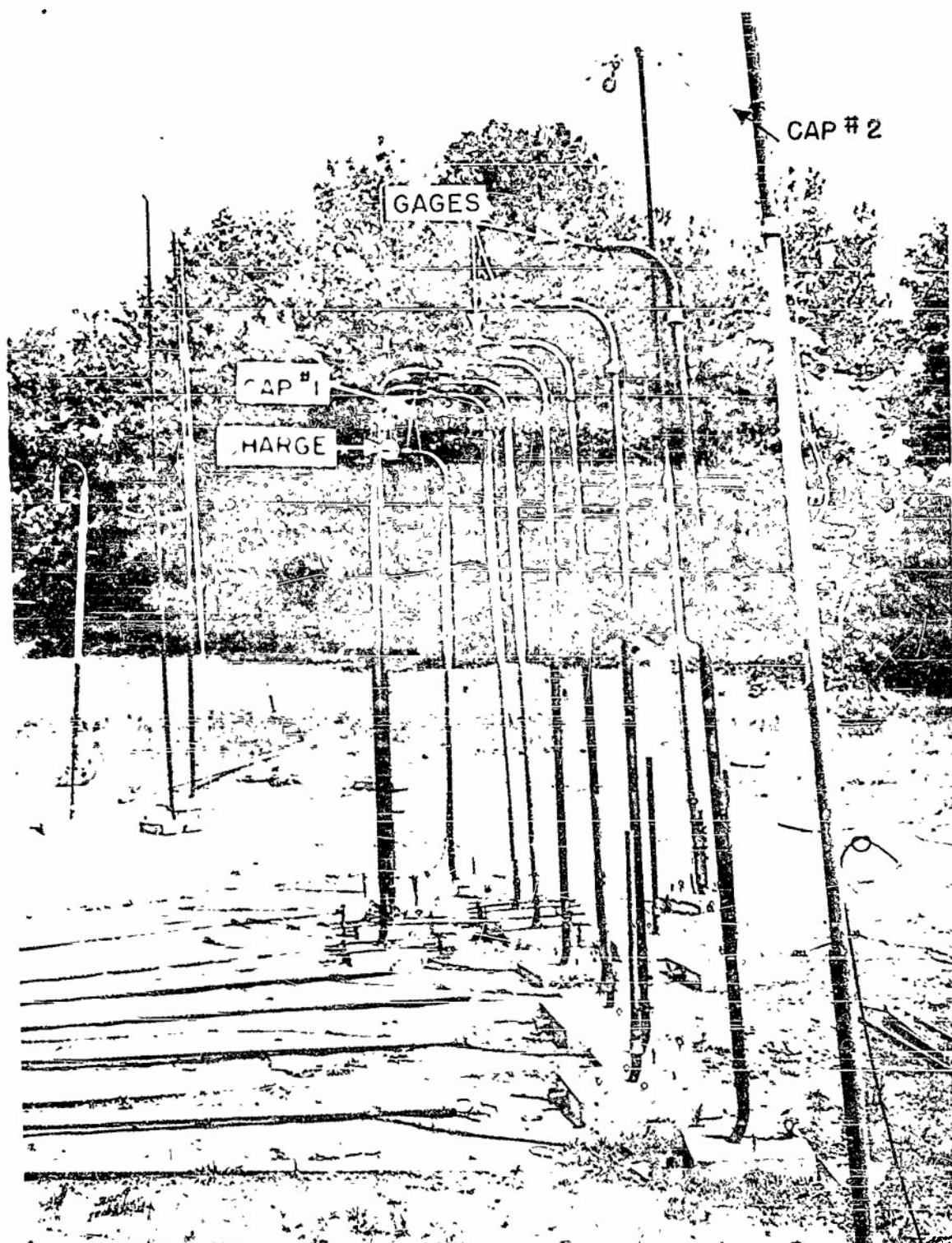


FIG. 3  
RELATIVE POSITION OF CHARGE, DETONATOR CAPS AND GAUGES

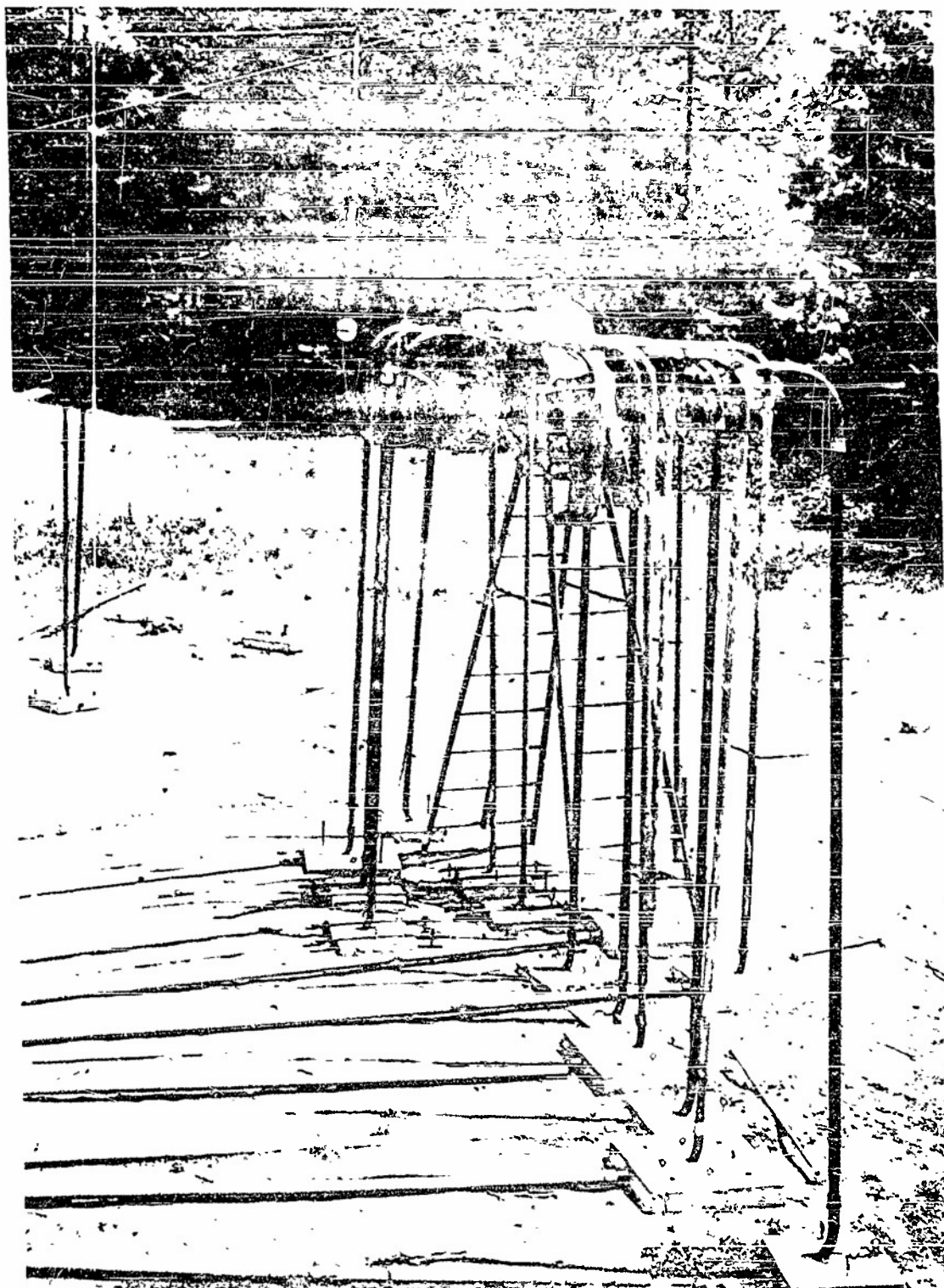


FIG.4 SPACING THE GAUGES



FIG. 5  
FIELD SET-UP  
(RELATIVE POSITION GAUGES, CAPS AND CHARGES)

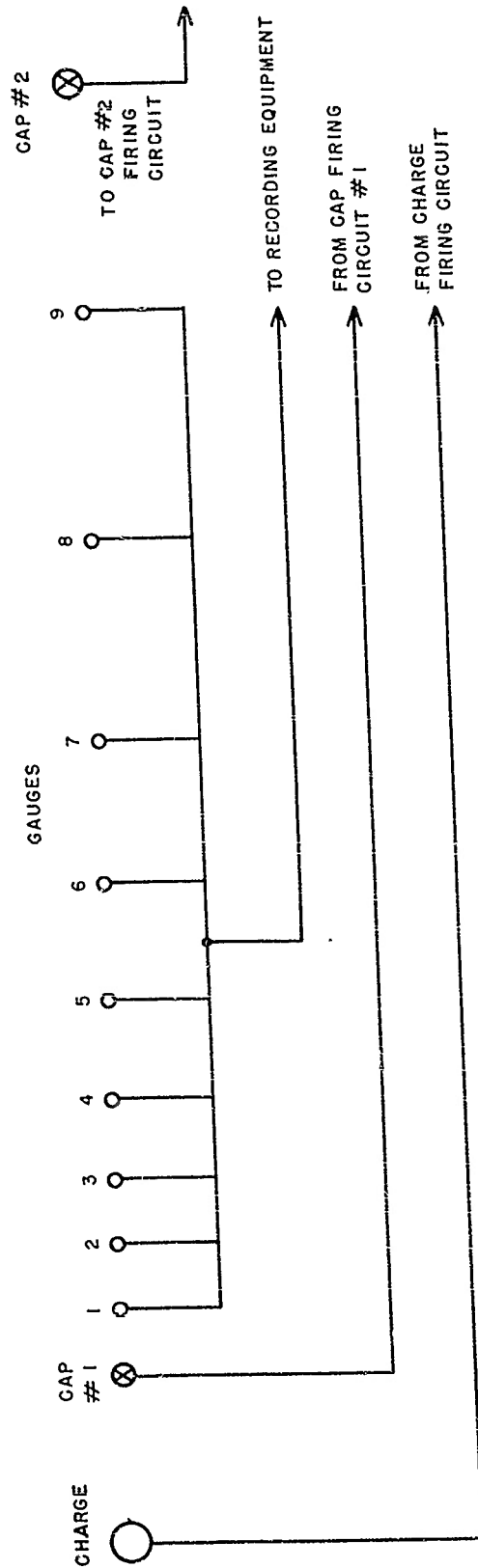






FIG. 6 INSERTING THE FIRING JUMPER

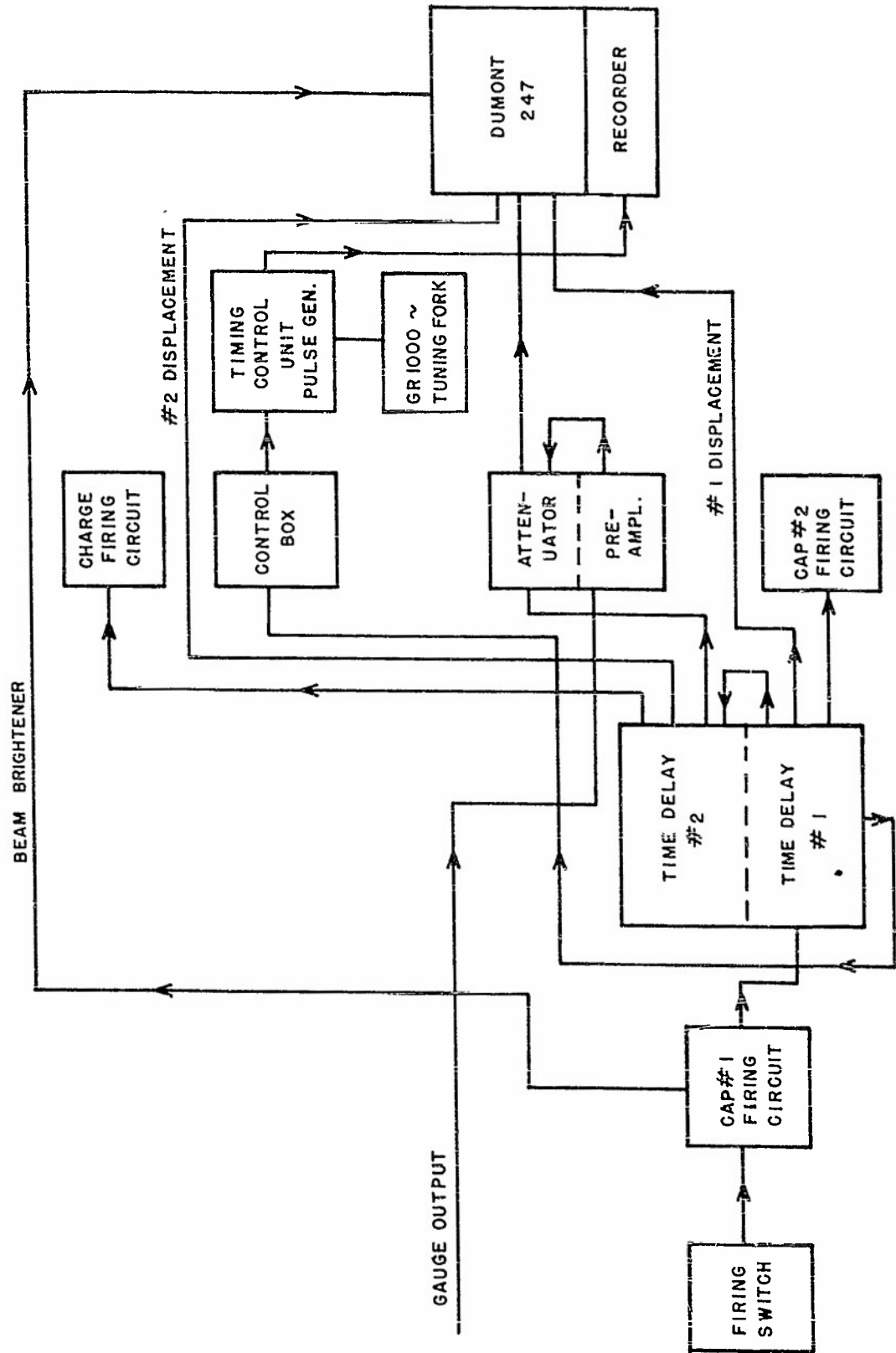
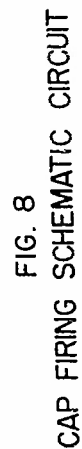


FIG. 7  
HIGH SPEED RECORDING EQUIPMENT



CI: STANGOR CHOKE C 1335  
L1: NEON READY LIGHT  
L2: PILOT LAMP  
S1: FIRING SWITCH

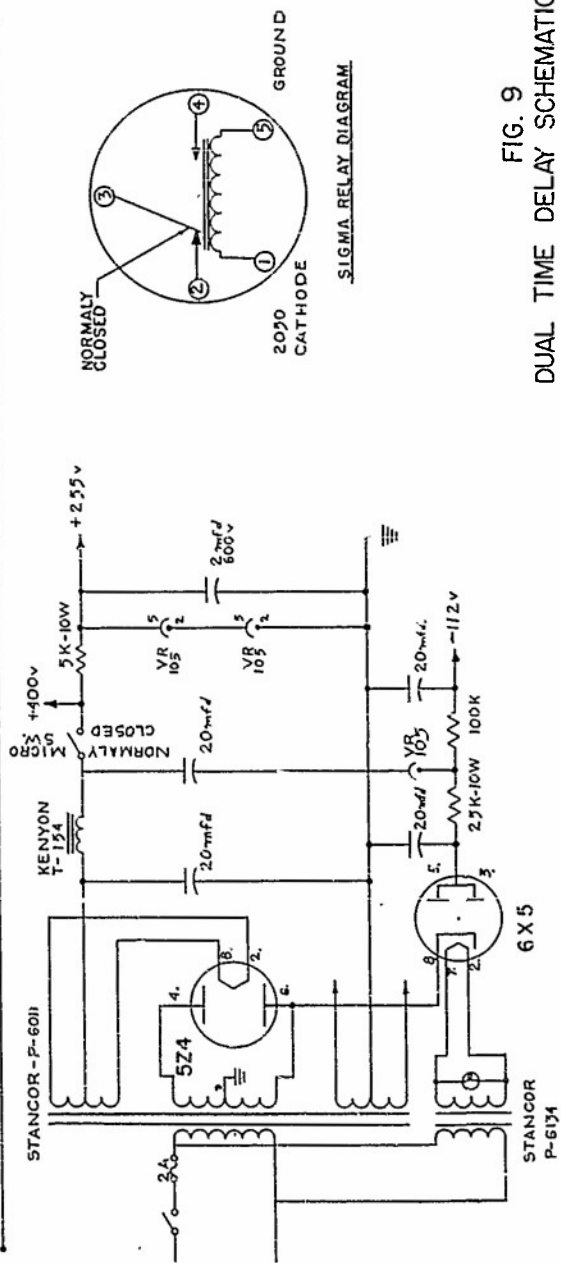
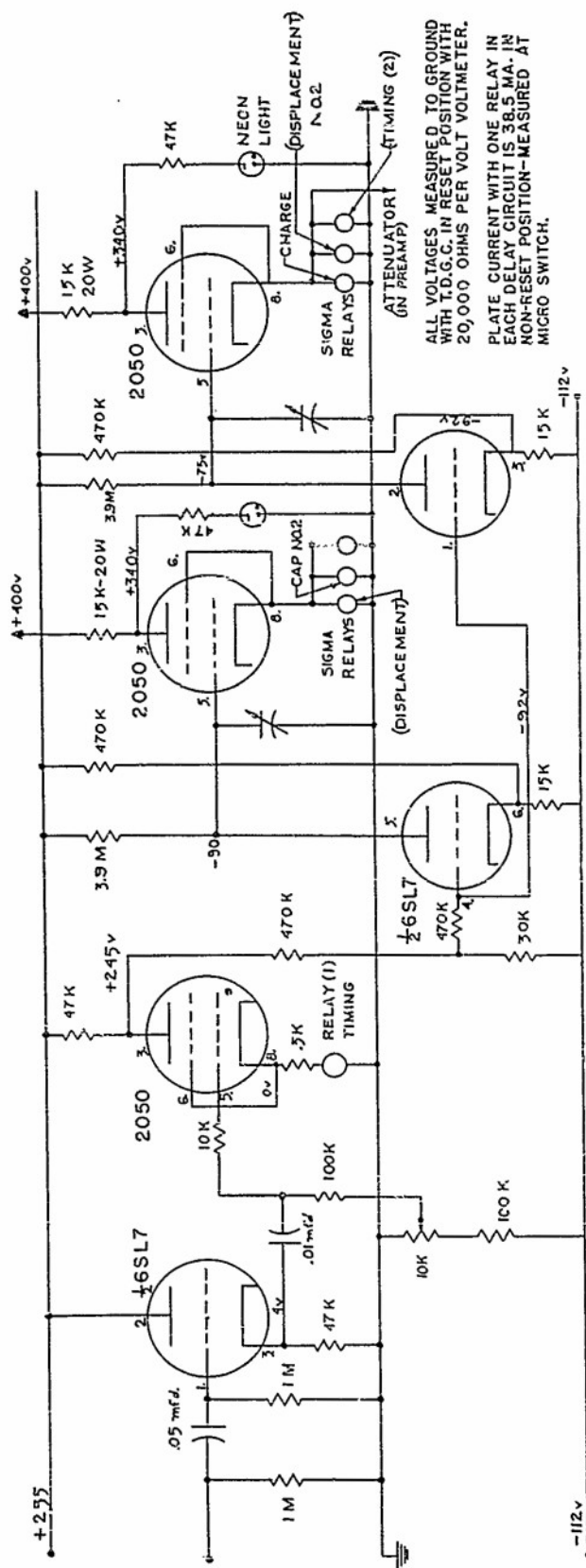


FIG. 9  
DUAL TIME DELAY SCHEMATIC CIRCUIT

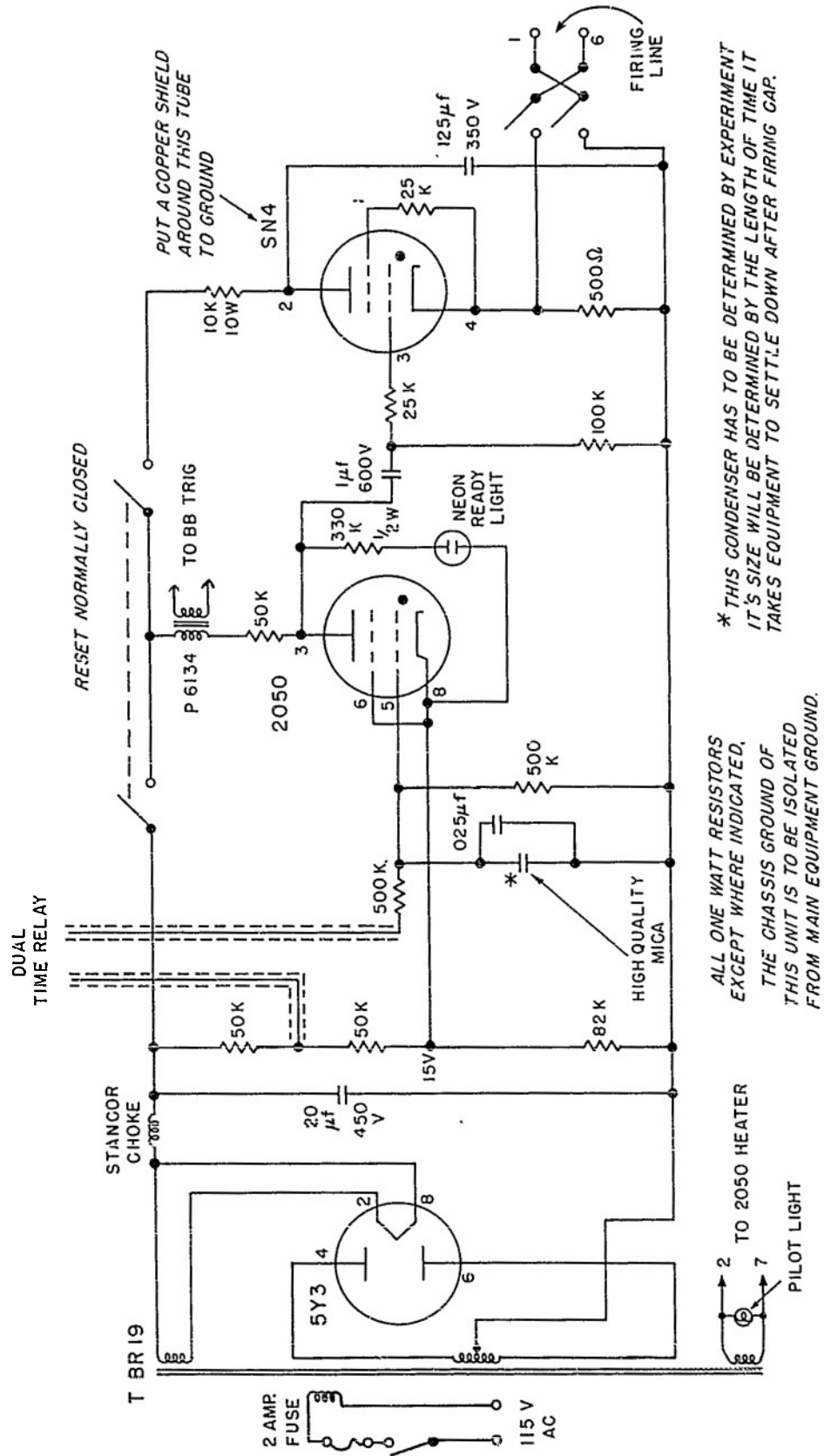


FIG. 10  
CHARGE FIRING CIRCUIT

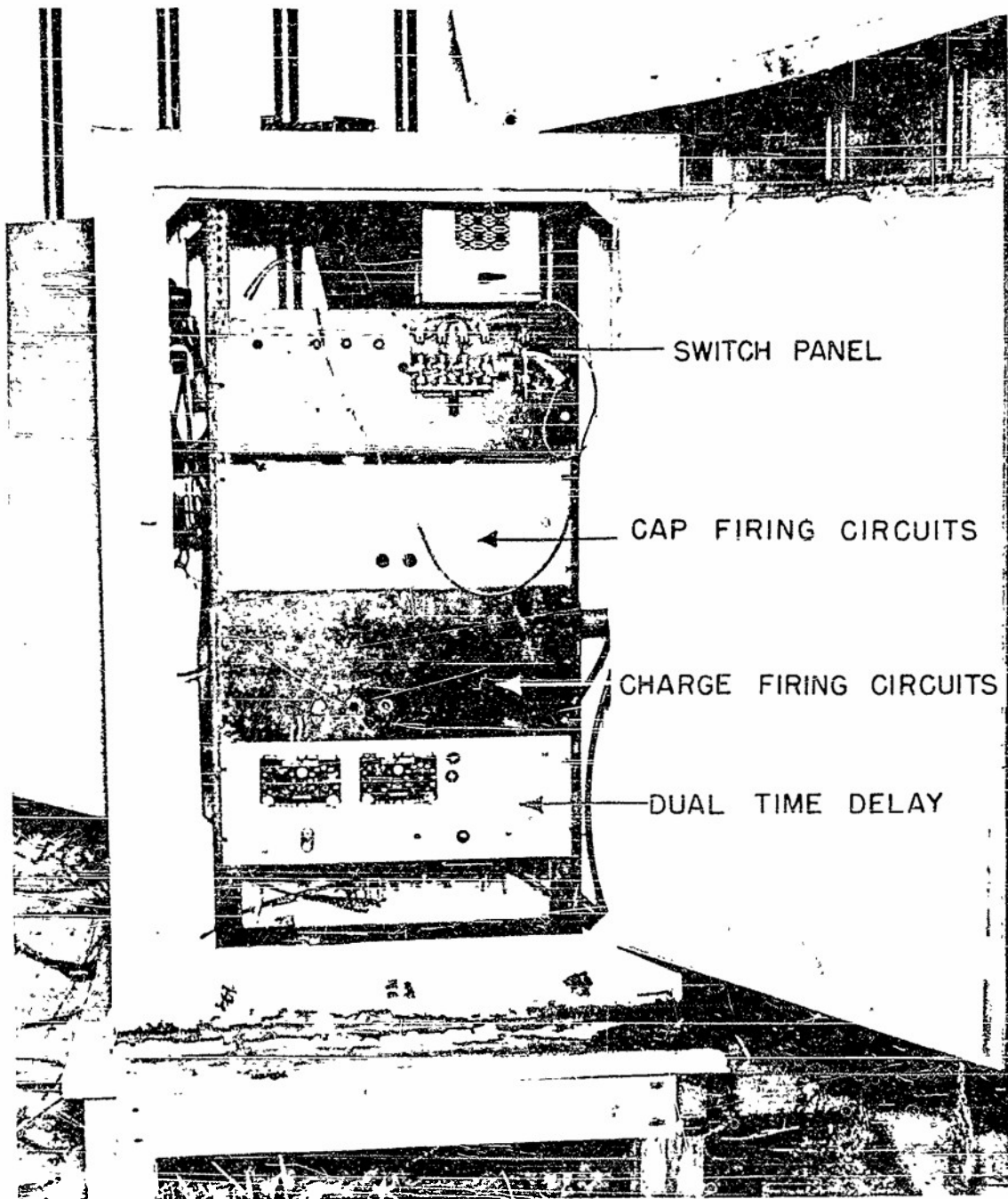
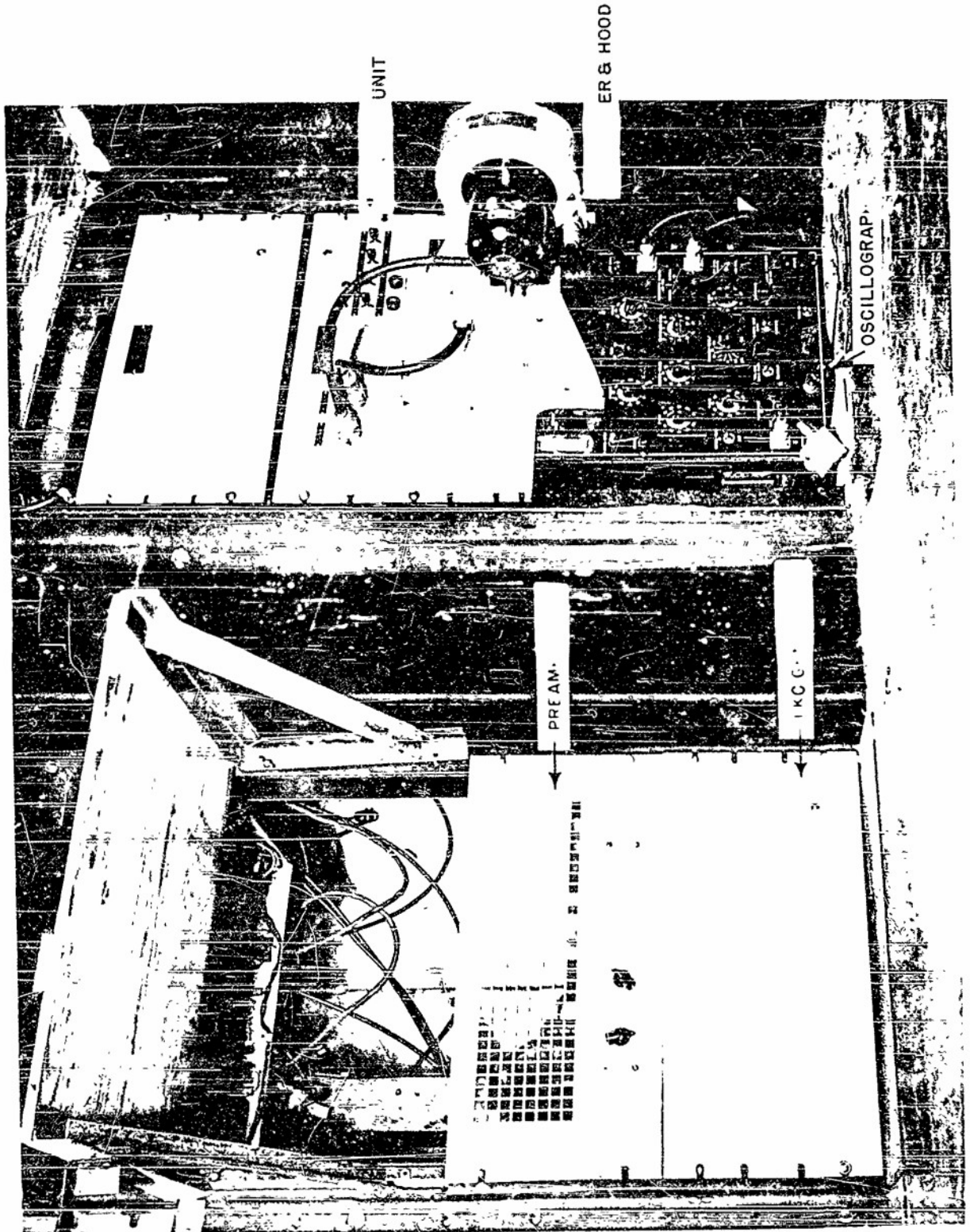
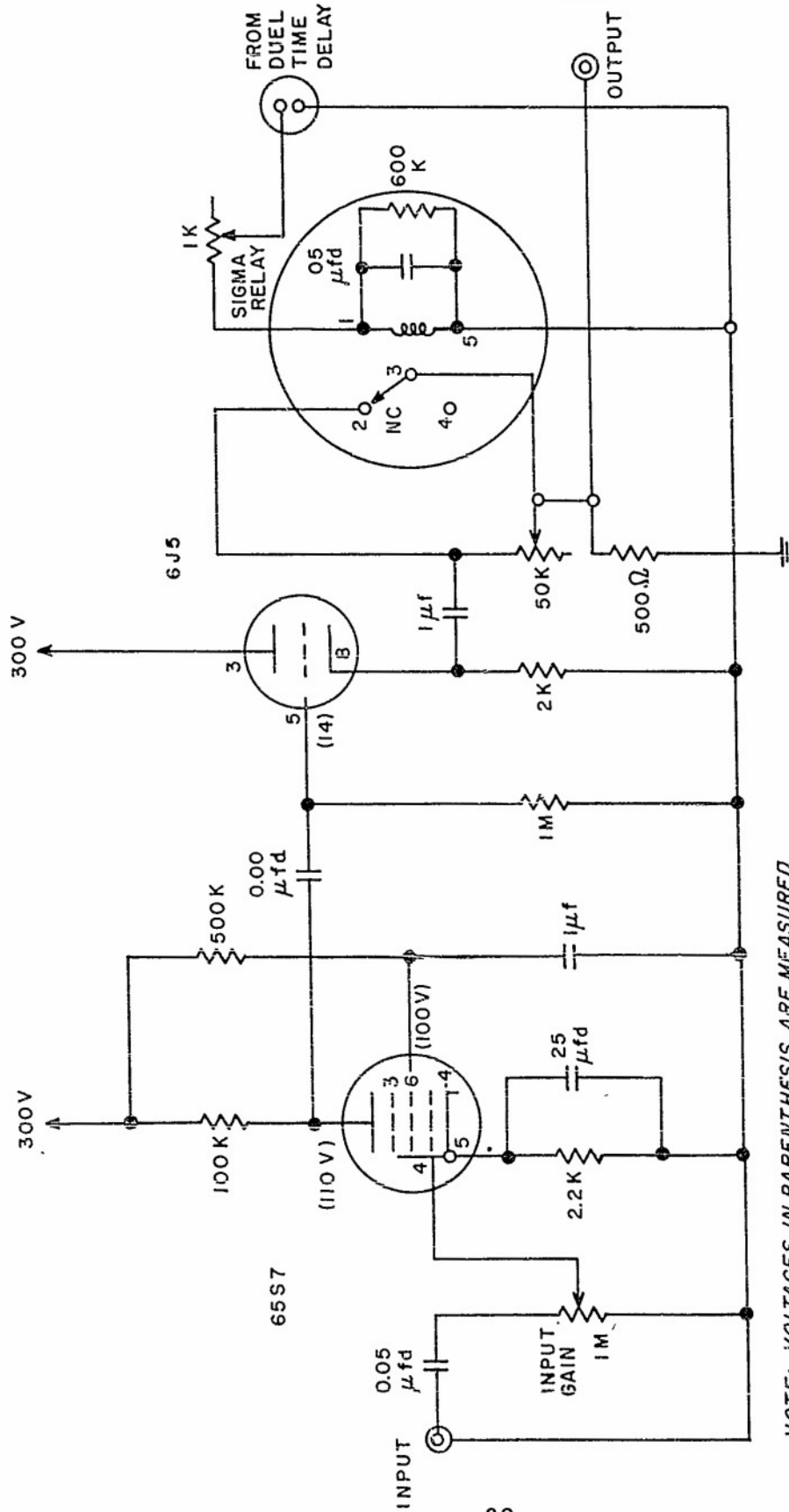


FIG.II FIRING AND DUAL TIME DELAY





NOTE: VOLTAGES IN PARENTHESIS ARE MEASURED TO GROUND.  
POWER SUPPLY TYPE 2 A #3 USED WITH THIS UNIT.

FIG. 13  
PRE-AMPLIFIER FOR HIGH SPEED RECORDING EQUIPMENT



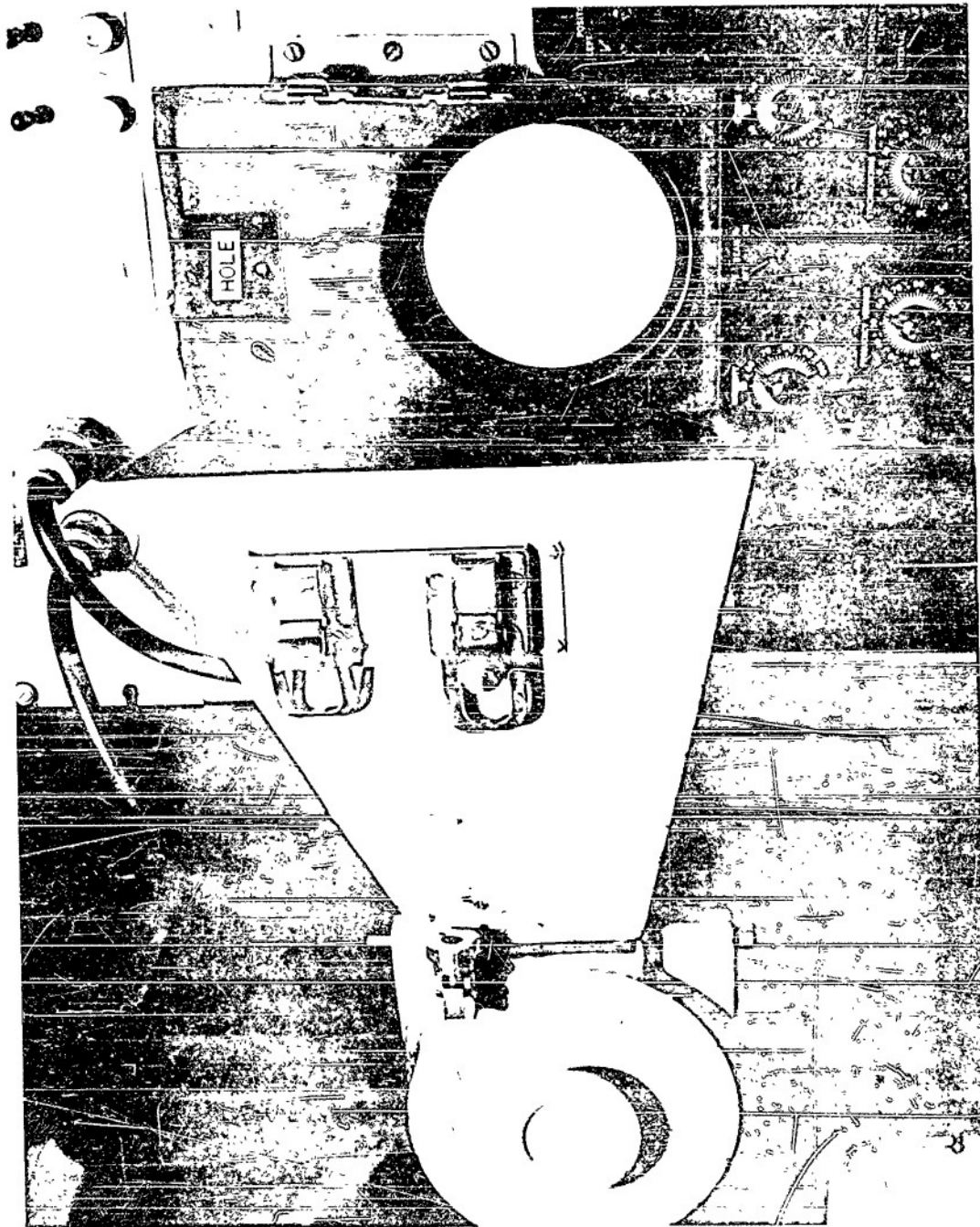


FIG. 14 HIGH SPEED RECORDER AND OSCILLOGRAPH SHOWING HOLE THROUGH WHICH CRATER TUBE FLASHING IS PHOTOGRAPHED

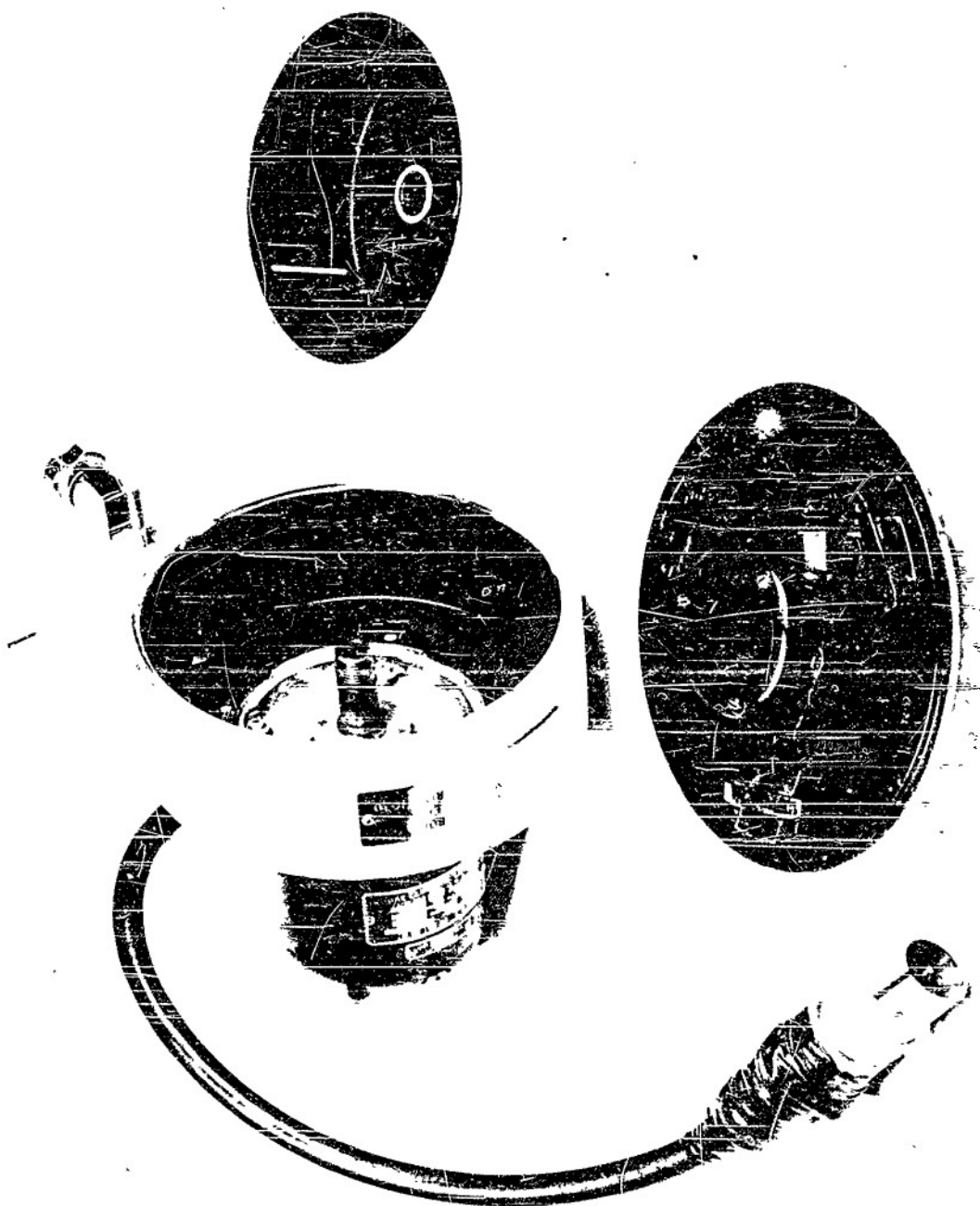


FIG. 15 DRUM FILM HOLDER

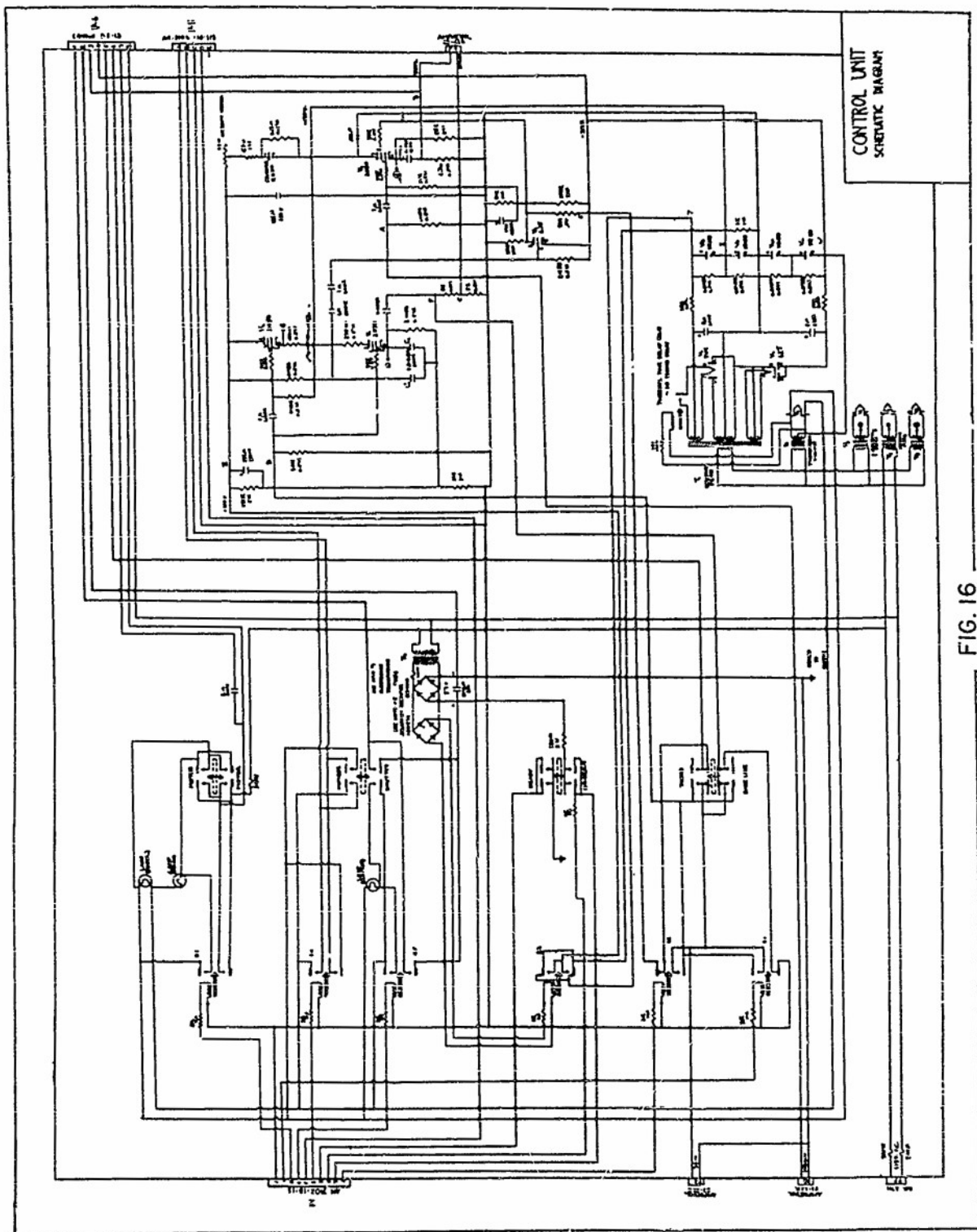


FIG. 16  
Control Unit Schematic Circuit

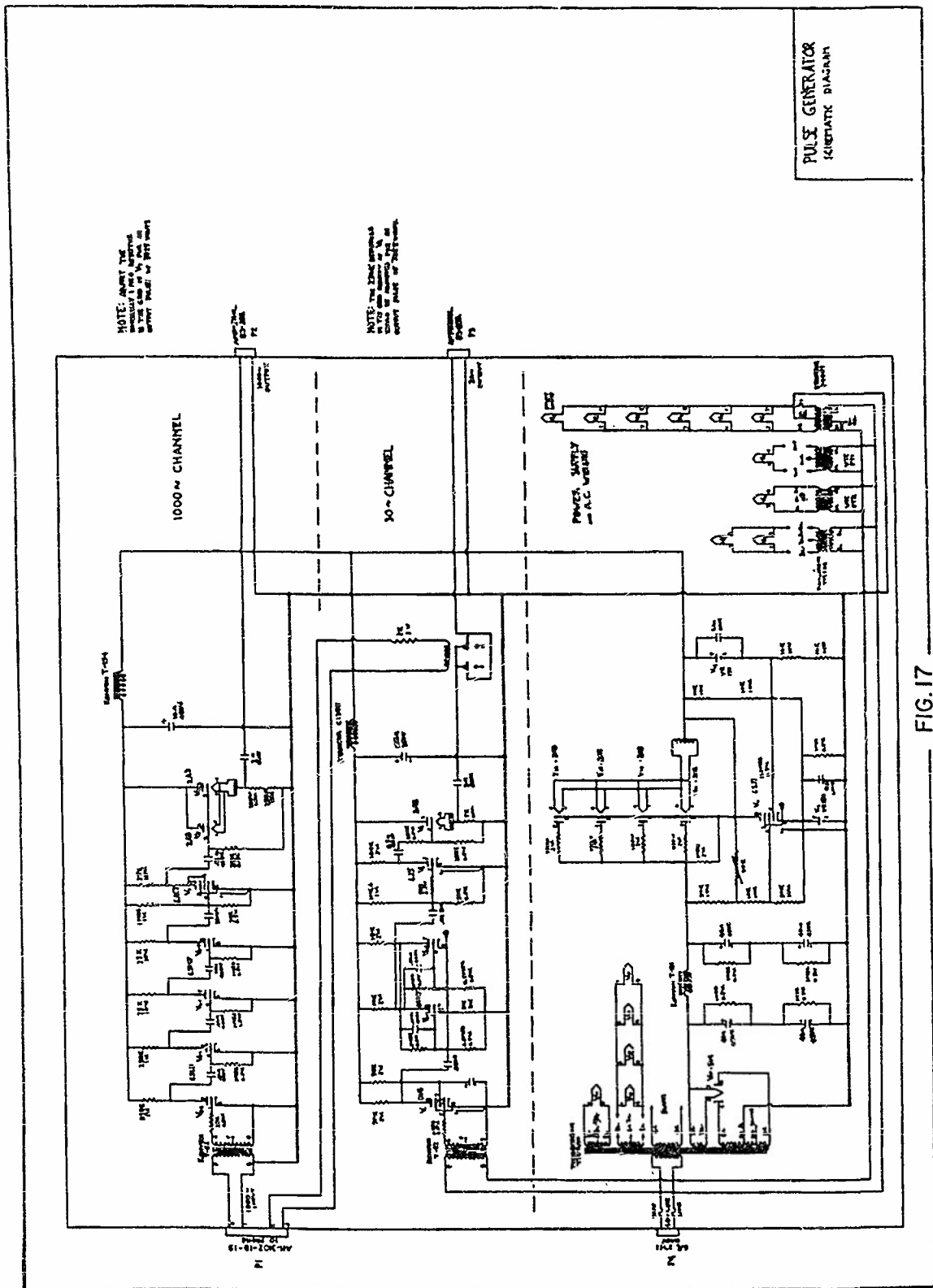


FIG. 17 Pulse Generator Schematic Circuit

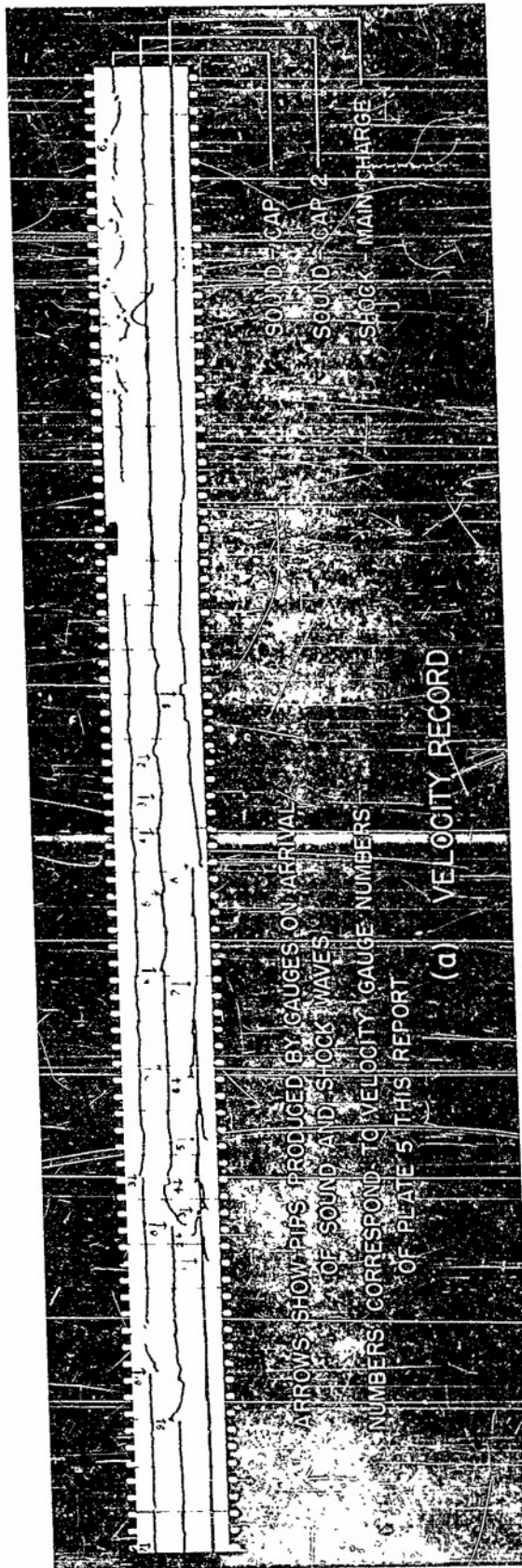


Fig. 18

REFERENCES

- (a) Instrumentation for Measurement of Underwater Pressures Generated by Explosives by Harry H. Hall, NAVORD Report 477.
- (b) Apparatus for the Measurement of Air Blast Pressures by Means of Piezo-electric Gauges by G. K. Fraenkel, NDRC Report No. A373, OSRD Report No. 6251.
- (c) Design and Use of Tourmaline Gauges for Piezo-electric Measurement of Air Blast by A. E. Arons and C. W. Tait, NDCR Report A-372, OSRD Report 6250.
- (d) The Behavior of the Shock Wave in Air From Small Underground Explosives, by Garth Stevens, NAVORD 1863.
- (e) Handbook of Chemistry and Physics, 30th Edition.
- (f) Theory and Application of Electron Tubes, by H. J. Reich, McGraw-Hill Book Company, Inc., New York, New York.
- (g) Resume of the Theory of Plane Shock and Adiabatic waves with applications to the Theory of the Shock Tube by C. W. Lampson, Report No. S-28174.

# NAVORD Report 2167

## DISTRIBUTION

|  |          |
|--|----------|
| Chief of the Bureau of Ordnance (Re2c) . . . . .   | 5 copies |
| Chief of Bureau of Aeronautics . . . . .   | 2 copies |
| Chief of Bureau of Medicine and Surgery . . . . .  | 2 copies |
| Chief of Bureau of Ships . . . . .   | 2 copies |
| Chief of Bureau of Yards and Docks . . . . .   | 2 copies |
| Chief of Naval Research . . . . .  | 2 copies |
| Chief of Ordnance, Department of the Army, Washington, D.C.  | 2 copies |
| Commanding General, Air Materiel Command, Wright Patterson<br>Field, Air Force Base, Dayton, Ohio . . . . .  | 2 copies |
|  |          |
| Commander, Naval Ordnance Test Station, Inyokern, California,<br>Post Office - China Lake, California . . . . .  | 3 copies |
| Director, Ballistic Research Laboratories, Aberdeen Proving<br>Ground, Maryland . . . . .  | 2 copies |
| Director, Naval Research Laboratory, Washington, D. C. . . .   | 2 copies |
| Chief, Armed Forces Special Weapons Program, The Pentagon,<br>Washington, D. C. . . . .  | 2 copies |
| Applied Physics Laboratory, Johns Hopkins University,<br>Silver Spring, Maryland VIA INM, Silver Spring, Maryland .                                    | 1 copy   |
| Dr. F. F. Cox, Sandia Corporation, Sandia Base,<br>Albuquerque, New Mexico VIA INM, Los Angeles 15, Calif. . .   | 1 copy   |
| Mr. E. Raynor, Assistant Chairman, Armour Research<br>Foundation, Illinois Institute of Technology, Chicago, Ill.<br>VIA INM, Chicago 11, Ill. . . . . | 1 copy   |
| Dr. E. B. Doll, Stanford Research Institute,<br>Stanford, California VIA INM, Los Angeles 15, California .   | 1 copy   |
| Frank A. Parker, Director, Project Squid, Princeton<br>University, Princeton, N. J. VIA INM, Newark, N. J. . . .                                       | 1 copy   |
| Los Alamos Scientific Laboratory, P. O. Box 1663,<br>Los Alamos, New Mexico VIA INM, Los Angeles 15, Calif. . .  | 2 copies |
| Mr. I. T. Watson, Waterway Experimental Station<br>P. O. 631, Vicksburg, Mississippi VIA INM, Atlanta 5, Ga.   | 1 copy   |
| Mr. W. L. Bowling, Waterway Experimental Station<br>P. O. 631, Vicksburg, Mississippi VIA INM, Atlanta 5, Ga. .  | 1 copy   |
| C. W. Lampson, BRL, Aberdeen Proving Grounds, Aberdeen, Md.  | 1 copy   |
| W. F. Curtis, BRL, Aberdeen Proving Grounds, Aberdeen, Md.   | 1 copy   |